

## Nickel Porphyrin Hybrid Material Based on Functionalised Silica for the Selective Oxidation of Benzyl Alcohol

Farook Adam\* and Ooi Wan-Ting

School of Chemical Sciences, Universiti Sains Malaysia  
11800 USM Pulau Pinang, Malaysia

\*Corresponding author: farook@usm.my

**Abstract:** Metalloporphyrin ligand, [tetrakis(o-chlorophenyl)porphyrinato]Ni(II) was successfully immobilised onto inorganic silica support from rice husk ash via 3-aminopropyltriethoxysilane (APTES) and the resulting catalyst was labeled RHAC-NiPor. This mesoporous organic-inorganic hybrid catalyst showed a high specific surface area of  $190.0 \text{ m}^2 \text{ g}^{-1}$ . The  $^{29}\text{Si}$  MAS NMR solid-state spectrum showed the presence of  $Q^4$ ,  $Q^3$ ,  $T^3$  and  $T^2$  silicon centres in RHAC-NiPor. The catalyst exhibited a good catalytic activity when used as a catalyst for the oxidation of benzyl alcohol with  $\text{H}_2\text{O}_2$ . A high selectivity to the desired product (benzaldehyde) of 100% and a maximum benzyl alcohol conversion of 54.9% was achieved. RHAC-NiPor could be reused several times without losing its catalytic activity.

**Keywords:** Metalloporphyrin, [tetrakis(o-chlorophenyl)porphyrinato]Ni(II), rice husk ash, 3-aminopropyltriethoxysilane, oxidation, benzyl alcohol

### 1. INTRODUCTION

Much effort has been devoted to the development of various environmental-friendly catalysts, especially organic-inorganic hybrid heterogeneous catalyst. With regards to this, a vast number of papers describing the synthesis of supported metalloporphyrin complexes for catalytic oxidation reactions have been published.<sup>1–5</sup> Although the unsupported metalloporphyrins exhibited a high catalytic performance for oxidation, epoxidation as well as hydroxylation reactions, they have a few limitations in the homogeneous system. For instance, self-destruction of catalyst happens during the course of reaction, and difficulty in separating as well as recovering from the reaction medium after the reaction for reuse.<sup>6,7</sup> Therefore, with the intention to overcome the above said disadvantages, many attempts have been made by immobilising metalloporphyrins onto a choice of different inorganic solid supports such as alumina, silica, polymers, zeolites, clays and resins.<sup>8–14</sup>

In recent years, the selective conversion of benzyl alcohol to chlorine-free benzaldehyde with high selectivity is of considerable importance in the

industry, because the latter is a versatile chemical widely used as a starting material in perfumery, cosmetic, pharmaceutical, dyestuff, flavouring and agro chemical industries.<sup>15,16</sup> Traditionally, oxidation of benzyl alcohol is carried out with the help of various hazardous and expensive inorganic oxidants, such as hypochlorite, manganese(IV) oxide, permanganate, chromium(IV) oxide and dichromate.<sup>17-21</sup> With growing environmental concern, clean oxidants like molecular oxygen and aqueous hydrogen peroxide are preferred as water is the only main side product of these reactions.

Numerous studies have been reported on the oxidation of benzyl alcohol to benzaldehyde by using different catalysts and oxidants under liquid phase condition.<sup>22-24</sup> Yang et al. reported the oxidation of benzyl alcohol using iodosylbenzene as oxidant.<sup>25</sup> It showed a very high catalytic activity with 100% conversion and selectivity towards benzaldehyde. The disadvantages of iodosylbenzene are low oxygen atom efficiency and high cost for practical application as compared to H<sub>2</sub>O<sub>2</sub>. Moreover, other promising catalysts such as palladium and gold supported on metal oxides have also been studied and they exhibited remarkable catalytic activity.<sup>26-28</sup> However, they are not cost effective.

Herein, we report the preparation of an organic-inorganic hybrid material by immobilising a metalloporphyrin complex, [tetrakis(*o*-chlorophenyl)porphyrinato]Ni(II) onto functionalised silica support obtained from rice husk (RH). In this work, we also report the catalytic activity of this hybrid material with respect to the liquid phase oxidation of benzyl alcohol using aqueous hydrogen peroxide as the green oxidant.

## 2. EXPERIMENTAL

### 2.1 Materials

The RH was obtained from a local rice mill in Penang. Nitric acid (65%) and sodium hydroxide (99%) were obtained from QReC. Propionic acid was purchased from HmbG Chemicals. Pyrrole and dichloromethane (DCM) (99%) were purchased from Merck. 3-Aminopropyltriethoxy silane (APTES) (98%) was purchased from Sigma Aldrich. Toluene and acetonitrile were purchased from J. T. Baker (99.8%). Benzyl alcohol was obtained from Unilab. All chemicals are AR grade and used as obtained without further purification.

### 2.2 Sources of Silica

Rice husk ash (RHA) was chosen as the source of amorphous silica from which the silica was extracted according to a previously reported method.<sup>29</sup>

### 2.3 Functionalisation of RHA with APTES

RHA silica was functionalised with APTES via a sol-gel reaction according to the method reported elsewhere<sup>30</sup> with some modification. About 3.0 g of RHA was stirred in 300 ml of 1.0 M NaOH at room temperature overnight. The sodium silicate formed was then filtered to remove undissolved particles. After that, APTES (6.0 ml, 0.026 mol) was added and the solution was titrated slowly with 3.0 M nitric acid until pH 3 with constant stirring. A white gel started to form when the pH decreased to less than 10. The gel formed was aged for 24 h at room temperature and then the gel was separated by centrifuge at 4000 rpm for 15 min (Rotina 38, Hittich Zentrifugn). This was repeated 5 times, with washing carried out using distilled water. Final washing was done with hot water. The sample was then dried in an oven overnight and it was ground to produce a fine powder. 3.45 g of RHACNH<sub>2</sub> was collected from this method and it was then used as the support to anchor the [tetrakis(*o*-chlorophenyl)porphyrinato]Ni(II).

### 2.4 Synthesis of [Tetrakis(*o*-chlorophenyl)porphyrinato]Ni(II)

For the synthesis of the metalloporphyrin complex, tetrakis(*o*-chlorophenyl)porphyrin was first synthesised according to the method reported by Alder-Longo<sup>31</sup> with some modification. 2-Chlorobenzaldehyde (20.3 ml, 0.18 mol) and pyrrole (12.5 ml, 0.18 mol) were added simultaneously to the refluxing propionic acid (1.5 l) and then the mixture was refluxed for 30 min. After cooling the mixture to room temperature, the precipitate formed was filtered and washed with an appropriate amount of cold methanol as well as hot water to give a violet solid of tetrakis(*o*-chlorophenyl)porphyrin. The synthesised tetrakis(*o*-chlorophenyl)porphyrin was then refluxed again with a small excess of nickel(II) chloride (molar ratio of 1:3) in dimethylformaamide (250 ml) for 4 h followed by stirring in an ice bath for another 2 h. An immediate precipitate of the complex [tetrakis(*o*-chlorophenyl)porphyrinato]Ni(II) was formed after an equal amount of cold distilled water was poured into the mixture and it was purified through recrystallisation technique in a 4:1 chloroform–methanol mixture. The product yield was 41.4%.

### 2.5 Preparation and Characterisation of RHAC-NiPor Catalyst

Preparation of the catalyst was carried out by a modified technique reported elsewhere.<sup>32</sup> The metalloporphyrin complex, [tetrakis(*o*-chlorophenyl)porphyrinato]Ni(II) (12.0 mmol) was added to a suspension of RHACNH<sub>2</sub> (3.0 g) in dry toluene (50 ml) and triethylamine (1.67 ml, 12.0 mmol). The reaction mixture was then allowed to reflux at 110°C in an oil bath for 24 h. The resulting solid was filtered and washed with toluene, DCM,

and distilled water followed by drying in an oven for 24 h. Finally, it was ground to a fine powder and 2.3 g of sample was obtained. The sample was labelled as RHAC-NiPor.

The catalyst was characterised by several spectroscopic and physical methods. These includes N<sub>2</sub> adsorption-desorption analysis, FTIR spectroscopy, X-ray diffraction analysis (XRD), Solid state <sup>29</sup>Si and <sup>13</sup>C nuclear magnetic resonance, transmission electron microscopy (TEM), scanning electron microscopy (SEM), image analyser and elemental analysis (CHN, EDX).

## 2.6 Oxidation of Benzyl Alcohol by H<sub>2</sub>O<sub>2</sub> using RHAC-NiPor

The liquid phase oxidation of benzyl alcohol was carried out in a 50 ml double neck round-bottom flask fitted with a water-cooled condenser. In a typical experiment, 10 mmol of benzyl alcohol, 10 ml of acetonitrile and 100 mg of catalyst were placed in the flask and heated in an oil bath with continuous stirring at 353K. After that, 10 mmol of dilute H<sub>2</sub>O<sub>2</sub> (30%) was added drop wise into the reaction flask and the reaction was carried out for the prescribed duration. 0.5 ml aliquot was withdrawn periodically each hour from the reaction mixture and 20 µl of cyclohexanone was added to the sample as the internal standard before GC and GC-MS analysis. After the reaction, the mixture was cooled and filtered to recover the catalyst. Percentage conversion of the reactant and the selectivity of the product was analysed by GC (PerkinElmer Clarus 500 with FID detector and a 30 m capillary wax column) while the organic product obtained was identified by using GC-MS (PerkinElmer Clarus 600 with the same column).

## 3. RESULTS AND DISCUSSION

### 3.1 Characterisation of Catalyst

#### 3.1.1 Nitrogen sorption analysis

Figure 1 shows the BET isotherms of RHACNH<sub>2</sub> and RHAC-NiPor. Both samples showed H<sub>2</sub> hysteresis loop which are usually observed for ink bottle shaped mesoporous material.<sup>33,34</sup> It can be observed that RHAC-NiPor maintained the characteristic of type IV isotherm and showed a uniform pore size distribution in the mesoporous region.

The N<sub>2</sub> sorption surface analysis parameters are listed in Table 1. RHACNH<sub>2</sub> has higher surface area and pore volume compared to RHAC-NiPor. The pore diameters of the catalyst decreased from 5.92 nm for RHACNH<sub>2</sub> to 4.90 nm for RHAC-NiPor after the immobilisation. Decrement in BET surface area,

pore volume, and pore diameter of the immobilised catalyst compared with that of RHACNH<sub>2</sub> confirmed that the metalloporphyrin complex are located within the pore channel of the support and thus resulted in the loss of partial inner surface of the support as well as blockage of some pore entrances by the metalloporphyrin complex moiety.<sup>35</sup>

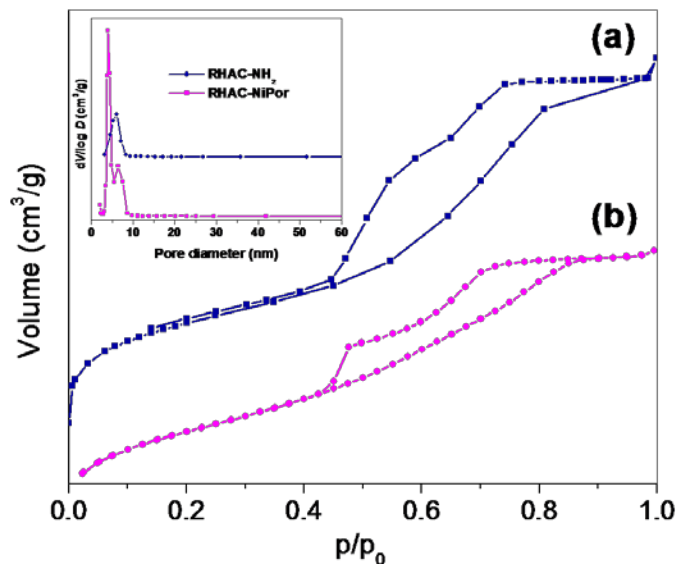


Figure 1: The N<sub>2</sub> adsorption-desorption isotherms and narrow pore size distribution (inset) of: (a) RHACNH<sub>2</sub> and (b) RHAC-NiPor.

Table 1: The result of BET analysis for RHACNH<sub>2</sub> and RHAC-NiPor.

Sample	Specific surface area ( $\text{m}^2 \text{g}^{-1}$ )	Average pore volume ( $\text{cm}^3 \text{g}^{-1}$ )	Average pore diameter (nm)
RHACNH <sub>2</sub>	253	0.343	5.92
RHAC-NiPor	190	0.209	4.90

### 3.1.2 FT-IR analysis

The IR spectra of RHA, RHACNH<sub>2</sub> and RHAC-NiPor are illustrated in Figure 2. Typically, a broad band with high intensity in the range of 3500–3400  $\text{cm}^{-1}$  corresponds to the O-H vibration of SiO-H groups and HO-H of adsorbed water. Meanwhile the bending vibration of the trapped water molecules in the silica matrix was detected at 1648  $\text{cm}^{-1}$ . The broad intense peak at 1089  $\text{cm}^{-1}$  in RHA was assigned to the asymmetric vibration of the siloxane bond, Si–O–Si associated with the condensed silica network in the silica and this value was shifted to 1107  $\text{cm}^{-1}$  and 1080  $\text{cm}^{-1}$  for RHACNH<sub>2</sub> and RHAC-NiPor,

respectively. The C–H stretching vibration can only be found in both RHACNH<sub>2</sub> and RHAC-NiPor at 2981 cm<sup>-1</sup> and 2935 cm<sup>-1</sup> respectively. Whereas stretching vibration of the C–N of primary amides appeared as an intense peak at 1378 cm<sup>-1</sup> and 1387 cm<sup>-1</sup> in RHACNH<sub>2</sub> and RHAC-NiPor. It can be seen that the intensity of this band decreased once the metalloporphyrin complex was incorporated onto the silica support. RHAC-NiPor also showed three additional peaks at 1638 cm<sup>-1</sup>, 1432 cm<sup>-1</sup> and 1315 cm<sup>-1</sup> which were ascribed to the transmission of C=C and C=N bonds of benzene and porphyrin ring. Transmission bands of the skeletal vibration of porphyrin ring were seen at 802 cm<sup>-1</sup>, 747 cm<sup>-1</sup> and 693 cm<sup>-1</sup> in RHAC-NiPor. These results prove the successful immobilisation of metalloporphyrin complex onto the silica support, RHAC-NH<sub>2</sub>.

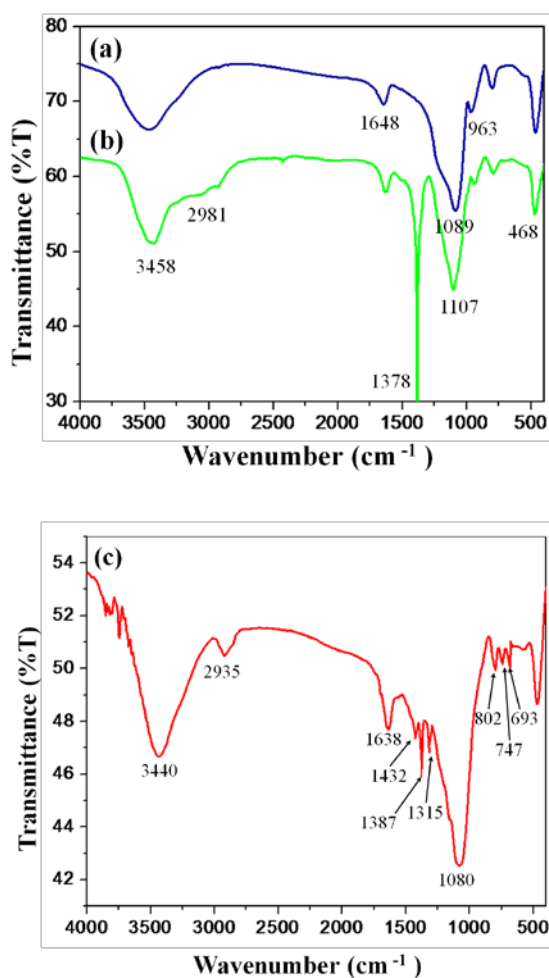


Figure 2: FT-IR spectra of (a) RHA, (b) RHACNH<sub>2</sub> and (c) RHAC-NiPor.

### 3.1.3 The X-ray diffraction analysis

The high angle XRD diffractogram of the catalyst is shown in Figure 3. The absence of diffraction peaks in the low angle XRD diffractogram of the catalyst indicates that this catalyst did not have any ordered pore arrangement. Whereas high angle XRD diffractogram of RHACNH<sub>2</sub> showed only one broad peak at around  $2\theta$  angle 22.5° due to the amorphous nature of the silica support and a slight shift of band to  $2\theta$  angle 23.7° was observed for RHAC-NiPor. This further proves that the immobilisation of tetrakis(*o*-chlorophenyl)porphyrinato Nickel(II) did not change the basic amorphous structure of silica and the metalloporphyrin complex was distributed homogeneously throughout the silica.

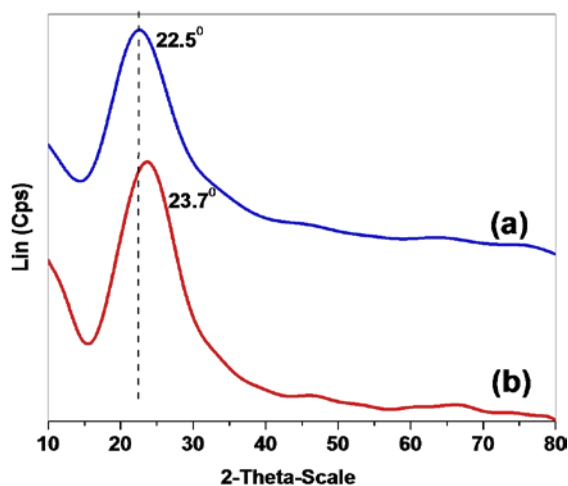


Figure 3: The X-ray diffraction pattern for (a) RHANH<sub>2</sub> and (b) RHAC-NiPor.

### 3.1.4 TEM and SEM analysis

The transmission electron micrographs (TEM) of RHACNH<sub>2</sub> and RHAC-NiPor are shown in Figure 4(a) and (b). The nano particles of RHACNH<sub>2</sub> appeared as a spherical shape with a diameter range of 20–40 nm while an enlargement of the particle size to 35–90 nm resulted in RHAC-NiPor. These nano particles overlapped with each other and arranged in a non-orderly manner.

SEM analysis of RHACNH<sub>2</sub> and RHAC-NiPor [Figure 4(c) and (d)] show the existence of granular particles with various sizes which were arranged randomly on the surface resulting in the porous surface of the material.

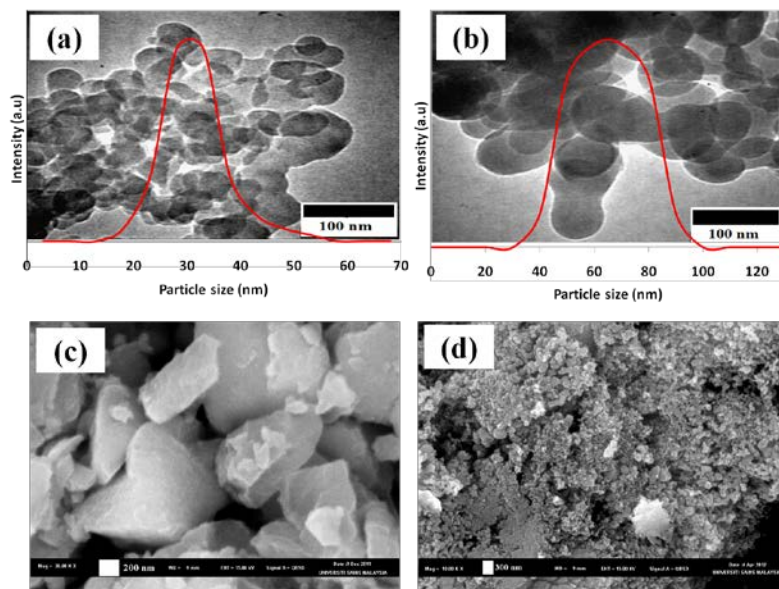


Figure 4: Particle size distribution of (a) RHACNH<sub>2</sub> and (b) RHAC-NiPor in the TEM images and SEM micrographs of (c) RHACNH<sub>2</sub> and (d) RHAC-NiPor.

### 3.1.5 Elemental analysis

Table 2 shows the elemental analysis of RHA, RHACNH<sub>2</sub> and RHAC-NiPor. The EDX analysis showed that nitrogen was only present in RHACNH<sub>2</sub> and RHAC-NiPor with the percentage of 5.61% and 8.06% respectively, which was as expected. RHAC-NiPor had 0.81% of Ni. As expected, the percentage of C and H for RHAC-NiPor was significantly higher than RHACNH<sub>2</sub>. The EDX analysis showed the presence of nickel in RHAC-NiPor from which we can conclude that the metalloporphyrin complex was successfully incorporated onto the functionalised silica support.

Table 2: Percentages of C, H and N obtained by elemental and EDX analysis for the RHA, RHACNH<sub>2</sub> and RHAC-NiPor.

Sample	Elemental analysis (%)				
	C	H	N	Si	Ni
RHA	(0.27)	(1.10)	–	36.66	–
RHACNH <sub>2</sub>	13.15 (6.27)	(2.44)	5.61 (2.36)	24.66	–
RHAC-NiPor	35.98 (44.17)	(12.91)	8.06 (6.83)	16.97	0.81

<sup>a</sup> Values in bracket were obtained by CHN analysis



### 3.1.6 $^{29}\text{Si}$ MAS NMR

The  $^{29}\text{Si}$  spectrum of  $\text{RHACNH}_2$  [Figure 5(a)] shows only the presence of  $\text{Q}^4$  ( $\text{Si}(\text{OSi})_4$ ) and  $\text{Q}^3$  ( $\text{Si}(\text{OSi})_3\text{OH}$ ) at  $\delta = -110.15$  and  $-101.28$  ppm respectively. These value had shifted to  $\delta = -93.21$  and  $-84.71$  attributed to  $\text{Q}^4$  and  $\text{Q}^3$  in  $\text{RHAC-NiPor}$  [Figure 5(b)]. A chemical shift at  $\delta = -66.93$  ppm for  $\text{RHACNH}_2$  indicates the formation of  $\text{Si-O-Si}$  linkages via three siloxane bonds, i.e.,  $(\text{SiO}_2)(-\text{O}-)_3\text{Si-CH}_2\text{CH}_2\text{CH}_2\text{-Por}$  ( $\text{T}^3$ ) and a chemical shift at  $\delta = -59.04$  ppm was attributed to the formation of two siloxane linkages, i.e.,  $(\text{SiO}_2)(-\text{O}-)_2\text{Si}(\text{OH})\text{CH}_2\text{CH}_2\text{CH}_2\text{-Por}$  ( $\text{T}^2$ ), to the silica.  $\text{RHAC-NiPor}$  also shows  $\text{T}^3$  and  $\text{T}^2$  chemical shifts at  $\delta = -50.37$  ppm and  $-41.30$  ppm respectively. The slight shift in the  $^{29}\text{Si}$  NMR spectrum of  $\text{RHAC-NiPor}$  with respect to  $\text{RHACNH}_2$  indicates the successful substitution at N of  $\text{RHACNH}_2$ , which essentially indicates the formation of the new C–N bond that immobilised the tetrakis(*o*-chlorophenyl)porphyrin onto the silica.

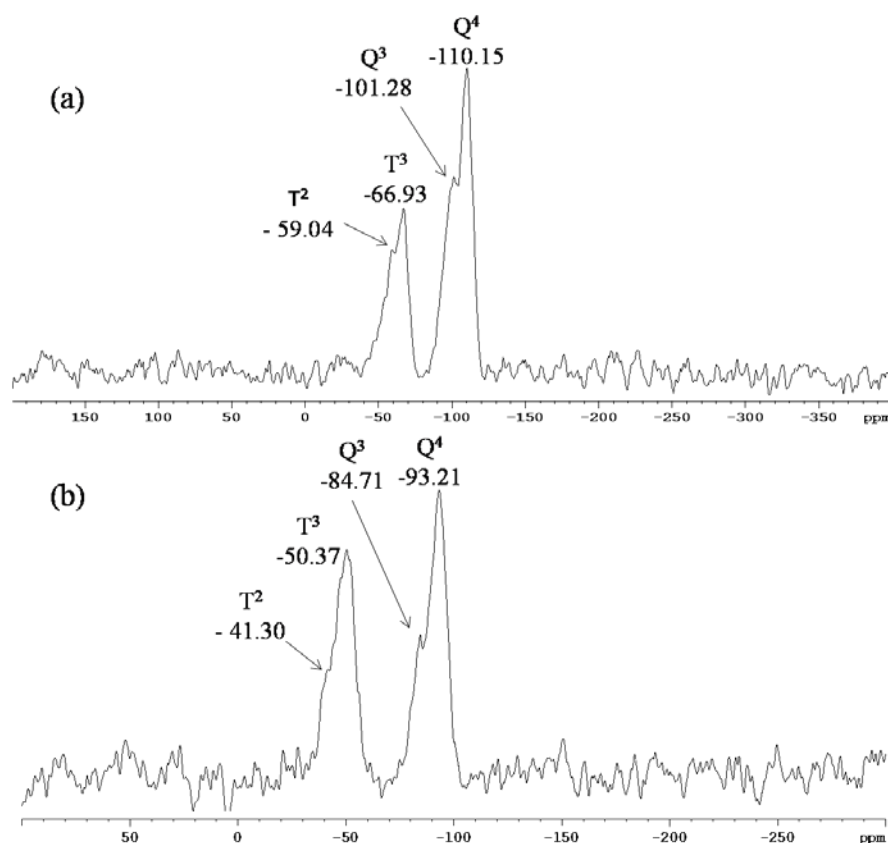
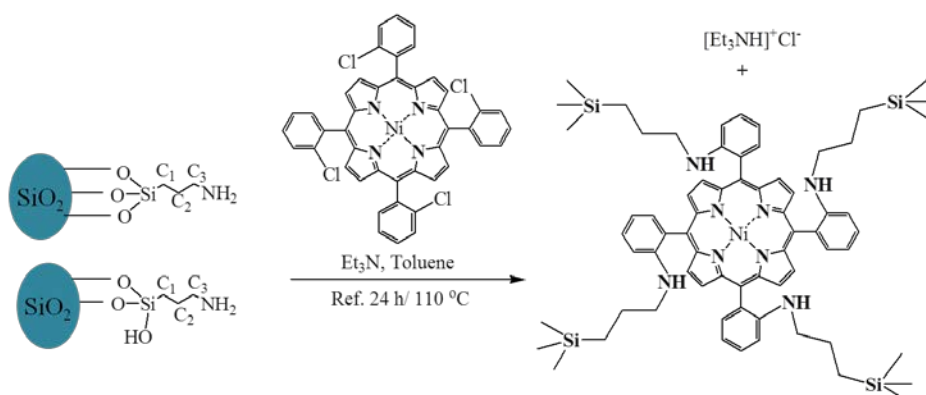


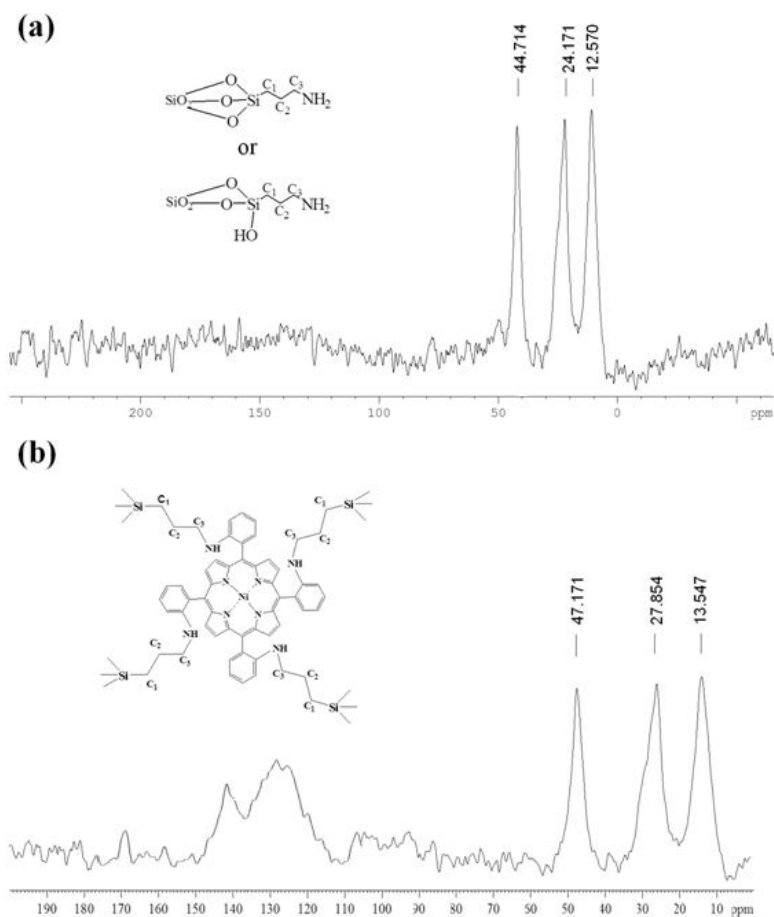
Figure 5:  $^{29}\text{Si}$  MAS NMR of (a)  $\text{RHACNH}_2$  and (b)  $\text{RHAC-NiPor}$ .

### 3.1.7 $^{13}\text{C}$ MAS NMR

More convincing information for the successful incorporation of tetrakis(*o*-chlorophenyl)porphyrinato nickel(II) onto RHACNH<sub>2</sub> support comes from  $^{13}\text{C}$  MAS NMR studies [(Figure (6)]. Generally, the incorporated propyl group (C<sub>1</sub>, C<sub>2</sub> and C<sub>3</sub>)<sup>36,37</sup> in RHACNH<sub>2</sub> appeared at chemical shifts,  $\delta = 12.57$  ppm, 24.17 ppm and 44.71 ppm, respectively. For RHAC-NiPor, these values were shifted to  $\delta = 13.55$  ppm, 27.85 ppm and 47.17 ppm respectively. A slight down field shift of the C<sub>3</sub> in RHAC-NiPor further verify the formation of new C–N bond which is in agreement with the result of  $^{29}\text{Si}$  NMR (Scheme 1). As can be observed in Figure 6(b), there is a broad chemical shift in the range of  $\delta = 100$ –170 ppm. These unresolved peaks were ascribed to the carbons of the metalloporphyrin complex. Therefore, taking into consideration all the analysis carried out on RHAC-NiPor, it can be concluded that tetrakis(*o*-chlorophenyl)porphyrinato nickel(II) was successfully incorporated onto the silica via the formation of new C–N bond. To the best of our knowledge, this is the first report detailing the  $^{13}\text{C}$  MAS NMR study for supported metalloporphyrin complexes.

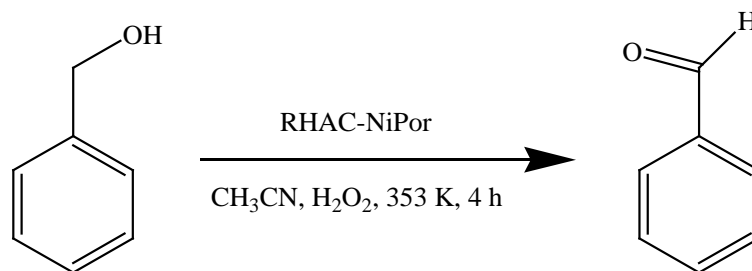


Scheme 1: The reaction sequence for the synthesis of RHAC-NiPor. The possible structure of the catalyst was postulated based on solid state ( $^{13}\text{C}$  and  $^{29}\text{Si}$ ) MAS NMR spectral studies.



### 3.2 Selective Oxidation of Benzyl Alcohol

The effectiveness of the prepared catalyst, (RHAC-NiPor) was tested in the liquid phase oxidation of benzyl alcohol. In order to optimise the reaction conditions, the reaction was carried out by varying several parameters such as the effect of reaction temperature, amount of catalyst and molar ratio of reactant over hydrogen peroxide used. The reusability of the catalyst was also determined. The optimum condition for this study show 100% selectivity towards the formation of benzaldehyde (Scheme 2).



Scheme 2: The oxidation of benzyl alcohol to benzaldehyde over RHAC-NiPor.

In general, temperature has a significant effect on the oxidation of benzyl alcohol. Hence, in this study, six different reaction temperatures in the range of 303K to 373K was tested and the results are shown in Table 3. The conversion of benzyl alcohol increased when the reaction temperature was increased and a maximum of 40.1% conversion was obtained at 353K. Raising the temperature accelerated the reaction as  $\text{H}_2\text{O}_2$  is more effectively consumed at higher temperature compared to that at low temperature.<sup>38</sup> However, further increase in the reaction temperature to 373K resulted in lower conversion. The reason for this decrease was due to the rapid thermal decomposition of  $\text{H}_2\text{O}_2$  at higher temperature which resulted in a relatively low activity.<sup>39</sup> Based on the results obtained, 353K was the optimum in terms of percentage conversion for the oxidation of benzyl alcohol with this catalyst.

Table 3: The effect of reaction temperature on the percentage conversion of benzyl alcohol and product selectivity.

Temperature (K)	Benzyl alcohol conversion (%)	Selectivity (%)	
		Benzaldehyde	Benzoic Acid
303	22.8	100	0
323	26.5	100	0
333	31.6	99.9	0.1
343	35.4	99.9	0.1
353	40.1	99.8	0.2
373	33.0	99.4	0.6

Reaction conditions: 80 mg RHAC-NiPor, molar ratio of substrate:  $\text{H}_2\text{O}_2 = 1:1$ , 10 ml  $\text{CH}_3\text{CN}$  solvent, 4 h of reaction.

In addition, the effect of catalyst weight was also investigated at 353K by using acetonitrile as the solvent for 4 h. As illustrated in Table 4, the sole product was benzaldehyde when 100 mg of catalyst was used and benzyl alcohol conversion increased from 30.7% to 54.2% when the mass of catalyst was increased from 30 mg to 100 mg. Lower conversion of benzyl alcohol into

benzaldehyde with smaller amount of catalyst used could be due to fewer catalytic sites.<sup>40</sup> On the other hand, the conversion decreased when the amount of RHAC-NiPor was increased to 150 mg. This phenomenon may possibly be due to the rapid decomposition of  $H_2O_2$  owing to the excessive catalytic sites. This is analogous to the rapid decomposition of  $H_2O_2$  at 373K. Therefore, 100 mg of RHAC-NiPor was the optimum weight of catalyst for the oxidation of benzyl alcohol under the system studied.

Table 4: Variation in benzyl alcohol conversion under different amount of catalyst studied.

Catalyst mass (mg)	Benzyl alcohol conversion (%)	Selectivity (%)	
		Benzaldehyde	Benzoic Acid
30	30.7	99.3	0.7
50	32.9	99.6	0.4
80	40.1	99.8	0.2
100	54.2	100	–
150	49.3	99.7	0.3

*Reaction conditions: 353K, molar ratio of substrate:  $H_2O_2 = 1:1$ , 10 ml  $CH_3CN$  solvent, 4 h of reaction.*

Table 5 presents the influence of benzyl alcohol and  $H_2O_2$  molar ratio on the catalytic activity. It is clear that, there is a steady increase in the conversion of benzyl alcohol with increase in  $H_2O_2$ . Nevertheless, the rate of benzyl alcohol conversion remained almost constant (54.2%, 54.9% and 54.5%) when the molar ratio of benzyl alcohol to  $H_2O_2$  was 1:1, 1:1.5 and 1:2. This could be due to an increasing amount of available oxygen liberated upon decomposition of  $H_2O_2$  when more  $H_2O_2$  resulting in a higher conversion of benzyl alcohol to benzaldehyde.<sup>16</sup> The selectivity of the products did not show significant variation as the molar ratio of benzyl alcohol to  $H_2O_2$  increased from 1:0.5 to 1:2. Thus, 1:1 molar ratio of benzyl alcohol to  $H_2O_2$  was taken to be an optimum molar ratio in this study.

Table 5: The effect of H<sub>2</sub>O<sub>2</sub> concentration on the oxidation of benzyl alcohol.

Benzyl alcohol:H <sub>2</sub> O <sub>2</sub> molar ratio	Benzyl alcohol conversion (%)	Selectivity (%)	
		Benzaldehyde	Benzoic Acid
1:0.5	41.5	99.8	0.2
1:1	54.2	100	–
1:1.5	54.9	99.9	0.1
1:2	54.5	100	–

Reaction conditions: 353K, 100 mg RHAC-NiPor, 10 ml CH<sub>3</sub>CN solvent, 4 h of reaction.

The recyclability of the catalyst was evaluated by running the reaction successively (under the optimum reaction conditions) over three recycles as shown in Table 6. The typical recycling procedure was as follows: after the initial reaction, the alcohol and catalyst was separated from the reaction medium by filtering and then the catalyst was regenerated by washing with distilled water and drying in an oven for few hours, followed by the activation at 110°C for 24 h. In three successive trials, the conversion and selectivity did not show significant difference. These results indicate that the catalyst could be easily recovered and used several times without significant loss in its catalytic activity.

Table 6: Reusability of RHAC-NiPor under optimised reaction conditions.

RHAC-NiPor	Conversion (%)
1st recycle	53.3
2nd recycle	51.8
3rd recycle	49

Reaction conditions: 353K, 100 mg RHAC-NiPor, molar ratio of substrate: H<sub>2</sub>O<sub>2</sub> = 1:1, acetonitrile (10 ml), 4 h.

The leaching test of the catalyst was carried out and the data obtained is shown in Table 7. The catalyst, RHAC-NiPor was removed after 1 h and the reaction was allowed to continue without the catalyst. It was noted that there was an increase of ca. 1.6% in conversion after the catalyst was removed until the end of the reaction at 4 h. Since the percentage increase is very small, thus this slight increment in benzyl alcohol conversion is most likely due to the concentration effect arising from evaporation during the transfer of reagents when filtering out catalyst from the reaction medium after 1 h. Hence, it can be concluded that leaching of nickel metal during the reaction in this study was insignificant.

Table 7: The leaching test of RHAC-NiPor.

Time (h)	Conversion (%)
1	20.9
2 <sup>a</sup>	21.8
3 <sup>a</sup>	22.2
4 <sup>a</sup>	22.5

Notes:

1. Reaction conditions: 353K, 100 mg RHAC-NiPor, molar ratio of substrate: H<sub>2</sub>O<sub>2</sub> = 1:1, acetonitrile (10 ml), 4 h of reaction.
2. <sup>a</sup> After removing the catalyst.

Literature review reveals that only a few studies have been made on the oxidation of benzyl alcohol by using nickel complex or modified nickel supported catalysts. Ali et al. reported a conversion of only 36% at 348K over 4 h.<sup>15</sup> While in the present case, RHAC-NiPor gives 54.9% conversion within the same period of time. Xavier et al. also reported a very low conversion of benzyl alcohol by using zeolite-encapsulated Ni(II) complex.<sup>41,42</sup> On the other hand, high conversion of benzyl alcohol (84%) was achieved by Mao et al.,<sup>43</sup> but it was achieved under severe conditions, like high temperature (653K). Nevertheless, their method yielded lower selectivity towards benzaldehyde compared with the present study which was 100% selectivity.

#### 4. CONCLUSION

In conclusion, a highly stable silica-supported metalloporphyrin complex was successfully synthesised, in which [tetrakis(*o*-chlorophenyl)porphyrinato]Ni(II) was successfully immobilised onto the functionalised silica support prepared from RHA. RHAC-NiPor can be used as an efficient catalyst for the liquid phase oxidation of benzyl alcohol with the environment friendly H<sub>2</sub>O<sub>2</sub> as a sole oxidant. The catalyst showed excellent catalytic activity with 100% selectivity towards benzaldehyde when 100 mg of RHAC-NiPor was used together with 1:1 benzyl alcohol to H<sub>2</sub>O<sub>2</sub> molar ratio at 353K for 4 h. Recycling of the catalyst indicates that the catalyst can be reused several times without significant loss in catalytic activity.

#### 5. ACKNOWLEDGEMENT

The authors would like to express their thanks to the Government of Malaysia for the RU grant (1001/PKIMIA/811092) and Universiti Sains Malaysia for a fellowship to author Ooi Wan-Ting.

## 6. REFERENCES

1. Rahiman, A. K. et al. (2009). Epoxidation of Styrene by Fe, Mn, and V metalloporphyrins encapsulated Si, Al, Ti And V- Mcm-41. *Catal. Lett.*, 127, 175–182.
2. Serwicka, E. M. et al. (2004). Cyclohexene oxidation by Fe-, Co-, and Mn-metalloporphyrins supported on aluminated mesoporous silica. *Appl. Catal. A*, 275(1–2), 9–14.
3. Ghiaci, M. et al. (2010). Metalloporphyrin covalently bound to silica. Preparation, characterization and catalytic activity in oxidation of ethyl benzene. *Catal. Commun.*, 11(8), 694–699.
4. Vartzouma, C. et al. (2007). Alkene epoxidation by homogeneous and heterogenised manganese(II) catalysts with hydrogen peroxide. *J. Mol. Catal. A: Chem.*, 263(1–2), 77–85.
5. Tangestaninejad, S. et al. (2002). Mn (Br8TPPS) supported on amberlite IRA-400 as a robust and efficient catalyst for alkene epoxidation and alkane hydroxylation. *Molecules*, 7(2), 264–270.
6. Mirkhani, V., Tangestaninejad, S. & Moghadam, M. (2003). Efficient oxidative decarboxylation of carboxylic acids with sodium periodate catalyzed by supported manganese(III) porphyrin. *Bioor. Med. Lett.*, 13(20), 3433–3435.
7. Sousa, A. N. et al. (2001). Manganeseporphyrin catalyzed cyclohexene epoxidation by iodobenzene: The remarkable effect of the meso-phenyl ortho-OH substituent. *J. Mol. Catal. A: Chem.*, 169(1–2), 1–10.
8. Rebelo, S. L. H., Goncalves, A. R. & Pereira, M. M. (2006). Epoxidation reactions with hydrogen peroxide activated by a novel heterogeneous metalloporphyrin catalyst. *J. Mol. Catal. A: Chem.*, 256(1–2), 321–323.
9. Połtowicz, J., Pamin, K. & Tabor, E. (2006). Metalloporphyrin complexes immobilized in zeolite NaX as catalysts of oxidation of cyclooctane. *Appl. Catal. A*, 299, 235–242.
10. Nakagaki, S., Halma, M. & Bail, A. (2005). First insight into catalytic activity of anionic iron porphyrins immobilized on exfoliated layered double hydroxides. *J. Colloid Interf. Sci.*, 281(2), 417–423.
11. Liu, S. T., Reddy, K. V. & Lai, R. Y. (2007). Oxidative cleavage of alkenes catalyzed by a water/organic soluble manganese porphyrin complex. *Tetrahedron*, 63(8), 1821–1852.
12. Nakagaki, S. et al. (2002). Immobilization of iron porphyrins into porous vycor glass: Characterization and study of catalytic activity. *J. Mol. Catal. A: Chem.*, 185(1–2), 203–210.
13. Nakagaki, S. et al. (2000). Synthesis and characterization of zeolite-encapsulated metalloporphyrins. *Colloids Surf. A*, 168(3), 261–276.



14. Poltowicz, J. & Haber, J. (2004). The oxyfunctionalization of cycloalkanes with dioxygen catalyzed by soluble and supported metalloporphyrins. *J. Mol. Catal. A: Chem.*, 220(1), 43–51.
15. Ali, S. R. et al. (2011). Synthesis of nickel hexacyanoferrate nanoparticles and their potential as heterogeneous catalysts for the solvent-free oxidation of benzyl alcohol. *Chin. J. Catal.*, 32(12), 1844–1849.
16. Ali, S. R. et al. (2009). Growth of zinc hexacyanoferrate nanocubes and their potential as heterogeneous catalyst for solvent-free oxidation of benzyl alcohol. *J. Mol. Catal. A: Chem.*, 303(1–2), 60–64.
17. Stevens, R. V., Chapman, K. T. & Weller, H. N. (1980). Convenient and inexpensive procedure for oxidation of secondary alcohols to ketones. *J. Org. Chem.*, 45(10), 2030–2032.
18. Holum, J. R. (1961). Study of the chromium(VI) oxide-pyridine complex. *J. Org. Chem.*, 26(12), 4814–4816.
19. Lee, D. G. & Spitzer, U. A. (1970). The aqueous dichromate oxidation of primary alcohols. *J. Org. Chem.*, 35(10), 3589–3590.
20. Highet, R. J. & Wildman, W. C. (1955). Solid manganese dioxide as an oxidizing agent. *J. Am. Chem. Soc.*, 77(16), 4399–4401.
21. Menger, F. M. & Lee, C. (1981). Synthetically useful oxidations at solid sodium permanganate surfaces. *Tetrahedron Lett.*, 22(18), 1655–1656.
22. Behera, G. C. & Parida, K. M. (2012). Liquid phase catalytic oxidation of benzyl alcohol to benzaldehyde over vanadium phosphate catalyst. *Appl. Catal. A*, 413(414), 245–253.
23. Jia, L. H. et al. (2012). Highly selective gas-phase oxidation of benzyl alcohol to benzaldehyde over silver-containing hexagonal mesoporous silica. *Microporous Mesoporous Mater.*, 149, 158–165.
24. Lei, Z. Q. & Wang, R. R. (2008). Oxidation of alcohols using H<sub>2</sub>O<sub>2</sub> as oxidant catalyzed by AlCl<sub>3</sub>. *Catal. Commun.*, 9(5), 740–742.
25. Yang, Z. W. et al. (2007). Oxidation of alcohols using iodosylbenzene as oxidant catalyzed by ruthenium complexes under mild reaction conditions. *J. Mol. Catal. A: Chem.*, 261(2), 190–195.
26. Harada, T. et al. (2007). A simple method for preparing highly active palladium catalysts loaded on various carbon supports for liquid-phase oxidation and hydrogenation reactions. *J. Mol. Catal. A: Chem.*, 268(1–2), 59–64.
27. Miedziak, P. J. et al. (2011). Oxidation of benzyl alcohol using supported gold–palladium nanoparticles. *Catal. Today*, 163, 47–54.
28. Ma, C. Y. et al. (2009). Catalytic oxidation of benzyl alcohol on Au or Au–Pd nanoparticles confined in mesoporous silica. *Appl. Catal. B*, 92(1–2), 202–208.

29. Adam, F. & Chua, J. H. (2004). The adsorption of palmytic acid on rice husk ash chemically modified with Al(III) ion using the sol-gel technique. *J. Colloid. Interface. Sci.*, 280(1), 55–61.
30. Adam, F., Hello, K. M. & Osman, H. (2010). Synthesis of mesoporous silica immobilized with 3-[(Mercapto or amino)propyl]trialkoxysilane by a simple one-pot reaction. *Chin. J. Chem.*, 28(12), 2383–2388.
31. Adler, A. D., Longo, F. R. & Finarelli, J. D. (1967). A simplified synthesis for mso-tetraphenylporphin. *J. Org. Chem.*, 32, 476.
32. Adam, F., Hello, K. M. & Osman, H. (2009). Esterification via saccharine mediated silica solid catalyst. *Appl. Catal. A*, 365(2), 165–172.
33. Adelkhani, H., Ghaemi, M. & Ruzbehani, M. (2011). Evaluation of the porosity and the nano-structure morphology of MnO<sub>2</sub> prepared by pulse current electrodeposition. *Int. J. Electrochem. Sci.*, 6(1), 123–135.
34. Pavasupree, S. et al. (2005). Synthesis, characterization and application of single and mixed oxides nanomaterials. *As. J. Energy Env.*, 6(4), 193–201.
35. Yang, Y. et al. (2011). Tethering of Cu(II), Co(II) and Fe(III) tetrahydro-salen and salen complexes onto amino-functionalized SBA-15: Effects of salen ligand hydrogenation on catalytic performances for aerobic epoxidation of styrene. *Chem. Eng. J.*, 171, 1356–1366.
36. Adam, F., Osman, H. & Hello, K. M. (2009). The immobilization of 3-(chloropropyl)triethoxysilane onto silica by a simple one-pot synthesis. *J. Colloid. Interf. Sci.*, 331(1), 143–147.
37. Bordoloi, A. et al. (2008). Inorganic-organic hybrid materials based on functionalized silica and carbon: A comprehensive understanding toward the structural property and catalytic activity difference over mesoporous silica and carbon supports. *Microporous Mesoporous Mater.*, 115(3), 345–355.
38. Chaudhari, M. P. & Sawant, S. B. (2005). Kinetics of heterogeneous oxidation of benzyl alcohol with hydrogen peroxide. *Chem. Eng. J.*, 106, 111–118.
39. Chang, F. et al. (2005). Highly selective oxidation of diphenylmethane to benzophenone over Co/MCM-41. *Chem. Lett.*, 34(11), 1540–1541.
40. Bansal, V. K., Thankachan, P. P. & Prasad, R. (2010). Oxidation of benzyl alcohol and styrene using H<sub>2</sub>O<sub>2</sub> catalyzed by tetraazamacrocyclic complexes of Cu(II) and Ni(II) encapsulated in zeolite-Y. *Appl. Catal. A*, 381, 8–17.
41. Xavier, K. O., Chacko, J. & Mohammed Yusuff, K. K. (2004). Zeolite-encapsulated Co(II), Ni(II) and Cu(II) complexes as catalysts for partial oxidation of benzyl alcohol and ethylbenzene. *Appl. Catal. A*, 258, 251–259.

42. Xavier, K. O., Chacko, J. & Mohammed Yusuff, K. K. (2002). Intrazeolite cobalt(II), nickel(II) and copper(II) complexes of 3-formylsalicylic acid for oxidation reactions. *J. Mol. Catal. A: Chem.*, 178, 275–281.
43. Mao, J. P. et al. (2009). Thin-sheet Ag/Ni-fiber catalyst for gas-phase selective oxidation of benzyl alcohol with molecular oxygen. *Catal. Commun.*, 10, 1376–1379.